

The energy distance for ensemble and scenario reduction

Florian Ziel

August 30, 2022

Abstract

Scenario reduction techniques are widely applied for solving sophisticated dynamic and stochastic programs, especially in energy and power systems. We propose a new method for ensemble and discrete scenario reduction based on the energy distance which is a special case of the maximum mean discrepancy (MMD). We discuss the choice of energy distance in detail, especially in comparison to the popular Wasserstein distance which is dominating the scenario reduction literature. The energy distance is a metric between probability measures which allows for powerful tests for equality of arbitrary multivariate distributions or independence. Thanks to the latter, it is a suitable candidate for ensemble and scenario reduction problems. The theoretical properties and considered examples indicate clearly that the reduced scenario set tend exhibit better statistical properties for energy distance than a corresponding reduction with respect to the Wasserstein distance. We show applications to binary trees and a real data based examples for electricity demand profiles.

keywords: energy score, Wasserstein metric, Kontorovic distance, scenario reduction, stochastic programming, electricity load, maximum mean discrepancy

1 Introduction and Motivation

In operations research and optimization literature ensemble and scenario reduction plays an important role for solving dynamic and stochastic programs. There are algorithms find an (approximately) optimal solution by valuating simulated trajectories/paths from uncertain process which are involved in the optimization problem. However, subsequent optimization steps are usually very costly in terms of computational effort - therefore ensemble or scenario reduction is applied. This holds especially with regards to applications for power and energy systems, see e.g. [Grove-Kuska et al. \(2003\)](#); [Wang et al. \(2008\)](#); [Leou et al. \(2013\)](#); [Di Somma et al. \(2018\)](#); [Biswas et al. \(2019\)](#); [Gazafroudi \(2019\)](#).

Based on a (weighted) set of simulated trajectories or paths a reduction technique is applied. The target for *ensemble reduction* is to find an *optimal* subset of m paths out of the simulated ensemble set with n paths where $m < n$, see Fig. 1a and 1b for illustration. Alongside with the classification also used in [Rujeerapaiboon et al. \(2017\)](#), in (discrete) *scenario reduction* (compare Fig. 1c) we aim to find next to the m subset paths the *optimal* associated probabilities. Thus, scenario reduction is usually a more sophisticated problem than ensemble reduction. Even more advanced, and related to clustering methods is *continuous scenario reduction* (see Fig. 1d). There we are looking for m new path and weights that approximate the target distribution well. Which method is required depends a lot on the underlying problem.

Obviously, the crucial question is: What means *optimal* in this context? In ensemble and scenario reduction literature, this is discussed and different criteria for optimality are suggested. An important selection criterion is the choice of a distance (or metric) which characterizes to

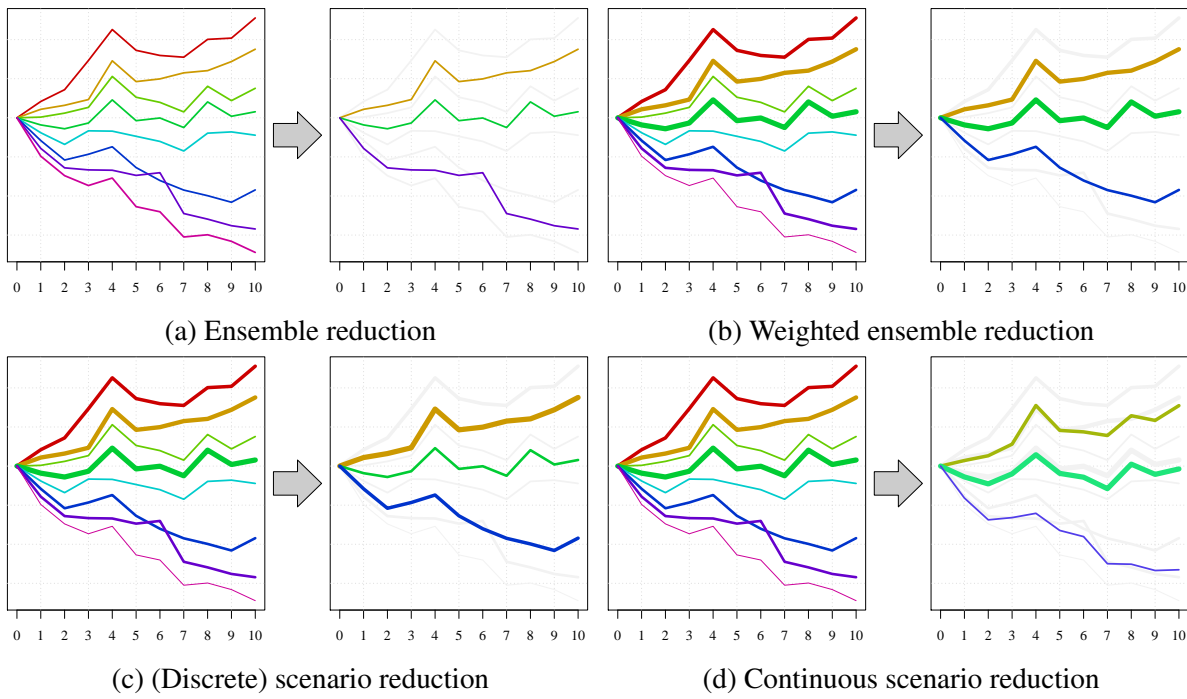


Figure 1: Illustration of ensemble and scenario reduction principles.

some extent close are the m selected trajectories to the considered large set of n trajectories in the scenario set.

The vast majority of articles favor the Wasserstein type distances resp. metrics (also Fortet-Mourier distance, Kantorovich/Kantorovich-Rubinstein distance, earth mover distance, optimal transport distance) for scenario reduction, see [Henrion et al. \(2009\)](#); [Rujeerapaiboon et al. \(2017\)](#); [Arpón et al. \(2018\)](#); [Glanzer and Pflug \(2020\)](#). This also holds for all applications mentioned in the first paragraph. The reason is mainly the fast scenario reduction method proposed by [Dupačová et al. \(2003\)](#), along with the implementation in the General Algebraic Modeling System (GAMS) by the function `Scenred`. It is based on the Wasserstein distance and the optimal redistribution rule (see e.g. [Grove-Kuska et al. \(2003\)](#)). It represents the reduction problem as a (mass) transportation problem with exhibits an explicit solution for the scenario reduction problem. As the Wasserstein distance is a metric for probability measure that additionally characterises weak convergence of measures it seems to be a suitable candidate for mentioned reduction problems. For instance [Rujeerapaiboon et al. \(2017\)](#) even state: '*The modern stability theory of stochastic programming indicates that the distance may serve as a natural candidate for this probability metric.*' in favor for the Wasserstein distance for scenario reduction problems.

However, there are reduction techniques which are not based on distances for probability measures, e.g. reduction techniques based on Euclidean distances, sampling or clustering [Beraldi and Bruni \(2014\)](#); [Keko and Miranda \(2015\)](#); [Davendra et al. \(2018\)](#); [Park et al. \(2019\)](#); [Zhou et al. \(2019\)](#). Still, from the theoretical point of view it makes sense to consider any ensemble or scenario reduction technique based on a probability metric as the scenario can be regarded as a (weighted) sample from a multivariate probability distribution.

In this article we propose an alternative to the Wasserstein type distances based reduction techniques. We propose the energy distance (sometimes referred as energy statistic) for ensemble and scenario reduction, see [Székely and Rizzo \(2013\)](#). The energy distance is a special case of the maximum mean discrepancy (MMD) which is popular in machine learning, see [Borgwardt et al. \(2006\)](#). In applications, it often shows preferable statistical/stochastic properties for reduction problems in contrast to Wasserstein distance based approaches. To motivate this more appropriately, we show a small toy example, illustrated in Figure 2.

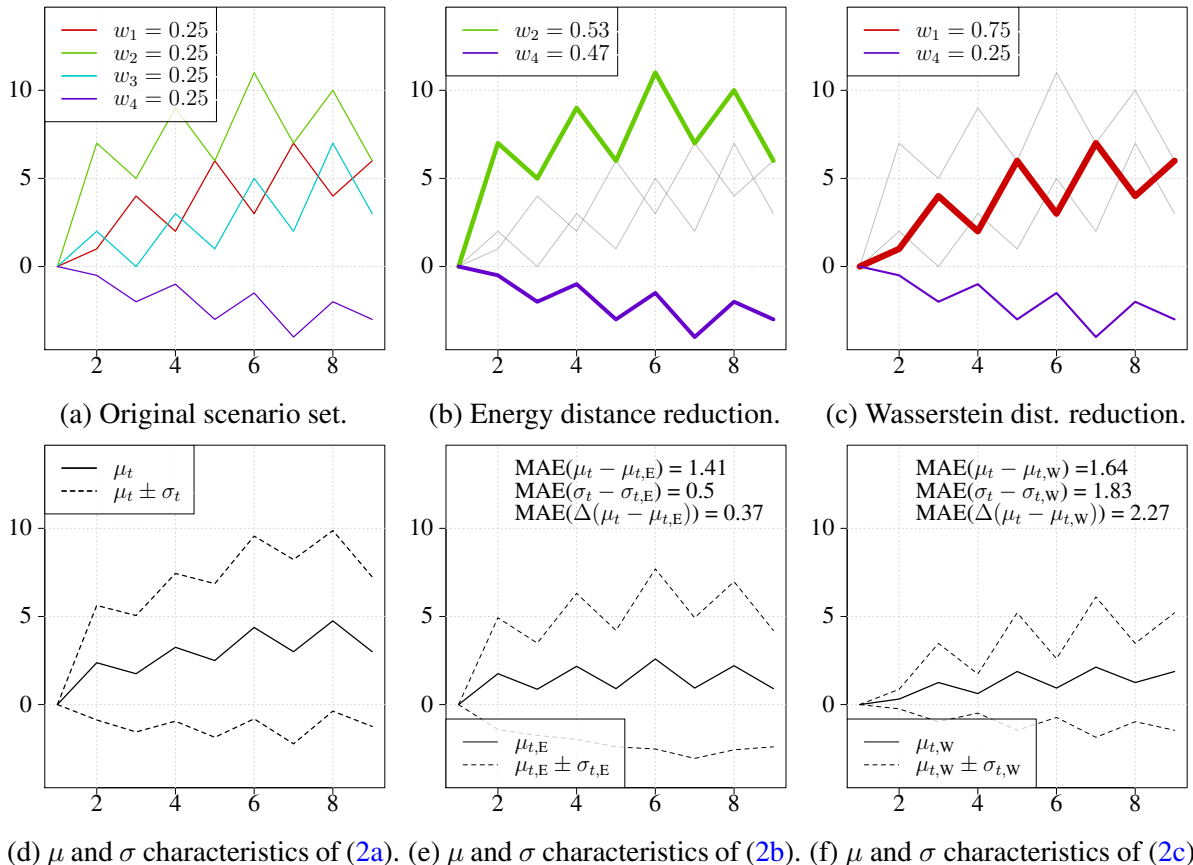


Figure 2: Illustration of scenario reduction example with 4 equally weighted scenarios which are reduced to 2 scenarios, containing the original setting (left), the reduction for the Energy distance (center) and Wasserstein distance (right). The top row shows the trajectories/paths with corresponding weights, the bottom row shows the illustrates mean μ and standard deviation σ .

Fig 2a shows the considered set of 4 scenarios $\mathbf{y}_1, \dots, \mathbf{y}_4$ on which we want to apply a scenario reduction so that the final set contains on 2 weighted trajectories. Figure 2d illustrates the main characteristics of the original ensemble, the first two moments with respect to the time dimension: Formally, the mean $\mu = \mathbb{E} \mathbf{Z}$ and standard deviation $\sigma = \sqrt{\text{diag}(\text{Cov } \mathbf{Z})}$ of the random variable $\mathbf{Z} = \frac{1}{4} \sum_{i=1}^4 \delta_{\mathbf{y}_i}$ with the Dirac mass δ . Figures 2b and 2c show the trajectories of the best scenario reduction for the energy distance and Wasserstein distance with corresponding weights. As in 2d, Figures 2e and 2f provides the mean and standard deviation of the reduction results with some approximation characteristics.

To understand the reduction results, first have a look at the considered scenario set. It contains 4 scenarios, first three of them tend to increase over time, the remaining trajectory 4 (purple) tends to decrease. Both scenario reduction techniques, eliminated two of the increasing trajectories in the optimal solution. The Wasserstein reduction is based on the optimal redistribution rule (see [Dupačová et al. \(2003\)](#)). In consequence the weights of the eliminated trajectories are redistributed to the remaining paths. In Figure 2c the weights of trajectories 2 (green) and 3 (cyan) are redistributed to trajectory 1 (red), with a final weight of 75%. On the first view this makes sense, as the trajectory 1 (red) tends to be the most centred one out of the three increasing trajectories. Indeed, if we would consider a classical transportation problem, this is the best choice. However, in many applications we use the remaining trajectories for sophisticated path-dependent optimization problems. Hence, we should care about the statistical/stochastic properties of the reduced scenario set. A method that transfers the full weight of a removed trajectory fully to another trajectory seem to be suboptimal. Moreover, in Figure 2a we observe that 3 out of 4 trajectories exhibit a zig-zag pattern with positive peaks at even time steps. Thus, the overall mean μ_t in Figure 2d shows the same behavior. Only trajectory 1 (red) deviates from this behavior and shows positive peaks at odd time steps. In the Wasserstein scenario reduction (see 2c) this trajectory 1 (red) got a high weight of 75%. As consequence, the corresponding mean exhibits peaks at odd time steps as well. Thus, this time series characteristic is not well covered at all, with likely huge negative consequences in decision making applications.

In contrast, the scenario reduction based on the energy distance (see Figures 2b and 2e) better preserves distributional properties which are usually relevant for decision making. The energy distance method keeps the trajectories 2 (green) and 4 (purple) with non-trivial weight assignment. It notices to some extend that trajectory 1 (red) does not show similar path dependencies to the remaining trajectories and decides for the alternative trajectory 2 (green) as a representative of the three increasing paths. Thus, the original zig-zag pattern of the mean μ_t is preserved in the mean $\mu_{t,E}$ of the reduced scenario set. When comparing quantitative measure, the mean absolute error (MAE) across t of the approximation of μ_t , σ_t and $\Delta\mu_t = \mu_t - \mu_{t-1}$ (see Figures 2e and 2f) we notice that in all characteristics the energy distance based scenario reduction is clearly favorable. Thus, it is worth to further investigate the energy distance for scenario reduction.

In the next section we introduce the considered setting for ensemble and scenario reduction. In section 3 we discuss of the energy distance and its properties which we compare with the the Wasserstein distance. Afterwards we show applications to binary tree and real power system data. We close a with a short discussion.

2 Basics and notations

Let $\mathcal{Y} = (\mathbf{y}_i)_{i \in \{1, \dots, n\}} = (\mathbf{y}_1, \dots, \mathbf{y}_n)$ with $\mathbf{y}_i \in \mathbb{R}^k$ be the large set of n k -dimensional scenarios with associated weights/probabilities $\mathbf{w} = (w_1, \dots, w_n)$ with $\mathbf{1}' \mathbf{w} = 1$ and $w_i \geq 0$. We may regard $(\mathcal{Y}, \mathbf{w})$ as weighted ensemble with associated random variable \mathbf{Y} which has the

(cumulative) distribution function

$$\mathbf{F}_Y(z) = \frac{1}{n} \sum_{i=1}^n w_i \mathbb{1}\{\mathbf{y}_i \leq z\}. \quad (1)$$

In the equally weighted case $\mathbf{w} = \frac{1}{n}\mathbf{1} = (\frac{1}{n}, \dots, \frac{1}{n})'$, \mathbf{y}_i can be regarded as a draw from the probability distribution \mathbf{F}_Y . In this situation \mathcal{Y} is usually referred as ensemble. If we encounter an application where $\mathbf{1}'\mathbf{w} = 1$ is not satisfied, we can achieve it by scaling.

In *weighted ensemble reduction*, we are looking for a suitable subset $\mathbf{c} = \{c_1, \dots, c_m\} \subseteq \{1, \dots, n\}$ with cardinality $\#(\mathbf{c}) = m \leq n$ and analyze the reduced subset $\mathcal{X} = \mathcal{X}(\mathbf{c}) = (\mathbf{x}_i)_{i \in \{1, \dots, m\}} = (\mathbf{y}_i)_{i \in \mathbf{c}} = (\mathbf{y}_{c_1}, \dots, \mathbf{y}_{c_m})$ of \mathcal{Y} with associated reduced weight vector $\mathbf{v} = \mathbf{v}(\mathbf{c}) = \frac{1}{s}(w_i)_{i \in \mathbf{c}} = (w_{c_1}, \dots, w_{c_m})/s$ with $s = \mathbf{1}'(w_i)_{i \in \mathbf{c}}$. The target is now to find \mathbf{c} so that $\mathbf{X} \sim \mathbf{F}_{\mathcal{X}}$ with distribution function

$$\mathbf{F}_X(z) = \frac{1}{m} \sum_{i=1}^m v_i \mathbb{1}\{\mathbf{x}_i \leq z\} \quad (2)$$

is close to $\mathbf{Y} \sim \mathbf{F}_{\mathcal{Y}}$ with respect to some distance or metric, see Figure 1a and 1b. If $\mathbf{w} = \frac{1}{n}\mathbf{1}$ we get $\mathbf{v} = \frac{1}{m}\mathbf{1}$ and refer this special case as *ensemble reduction* (see Fig. 1a). Therefore, let $d(\cdot, \cdot)$ be a distance (or metric) between two k -dimensional random variables. Examples are the Wasserstein or energy distance which is discussed more detail the next section.

To recap, the given weighted set of n scenarios $(\mathcal{Y}, \mathbf{w})$ is going to be reduced to $(\mathcal{X}, \mathbf{v}) = ((\mathbf{y}_i)_{i \in \mathbf{c}}, (w_i)_{i \in \mathbf{c}})$ with $m \leq n$ scenarios corresponding to the subset $\mathbf{c} \subseteq \{1, \dots, n\}$. Formally, this reduction problem can be written as a minimization:

$$\mathbf{c}_{\text{opt}}(\mathcal{Y}, \mathbf{w}, m) = \arg \min_{\mathbf{c} \subseteq \{1, \dots, n\}, \#(\mathbf{c})=m} d(\mathbf{X}(\mathbf{c}; \mathcal{Y}, \mathbf{w}), \mathbf{Y}(\mathcal{Y}, \mathbf{w})). \quad (3)$$

with $\mathbf{X}(\mathbf{c}; \mathcal{Y}, \mathbf{w}) \sim \mathbf{F}_X$ and $\mathbf{Y}(\mathcal{Y}, \mathbf{w}) \sim \mathbf{F}_Y$ as defined in (2) and (1). Then $((\mathbf{y}_i)_{i \in \mathbf{c}_{\text{opt}}}, (w_i)_{i \in \mathbf{c}_{\text{opt}}})$ is the optimally reduced ensemble with respect to d . In general, (3) is an NP-hard problem due to the combinatorial complexity. Thus, only in small dimensional cases we can guarantee to find the optimal solution.

Scenario reduction is a generalization of the weighted ensemble reduction. We are looking to the optimal subset \mathbf{c} with a given cardinality and for optimal weights $\mathbf{a} = (a_i)_{i \in \mathbf{c}} \in \mathbb{R}^m$. They are chosen so that the reweighted reduced ensemble $(\mathcal{X}, \mathbf{a})$ approximates well the original weighted scenario set $(\mathcal{Y}, \mathbf{w})$ with respect to a distance d (see Fig. 1c). The scenario reduction problem is usually solved by having an inner continuous optimization for the weights \mathbf{a} and an outer optimization for \mathbf{c} which corresponds to an integer-valued optimization, see e.g. [Rujeera-paiboon et al. \(2017\)](#). Denote $\mathcal{C}_n(m) = \{\mathbf{c} | \mathbf{c} \subseteq \{1, \dots, n\}, \#(\mathbf{c}) = m\}$ the set of all subset of $\{1, \dots, n\}$ with cardinality m . Then optimization procedure for a target cardinality m can be written as

1. For all $\mathbf{c} \in \mathcal{C}_n(m)$ solve

$$\mathbf{a}(\mathbf{c}) = \arg \min_{\mathbf{a} \in [0, 1]^m, \mathbf{a}'\mathbf{1}=1} d(\mathbf{X}(\mathbf{c}; \mathcal{Y}, \mathbf{a}), \mathbf{Y}(\mathcal{Y}, \mathbf{w})) \quad (4)$$

with $\mathbf{X}(\mathbf{c}; \mathcal{Y}, \mathbf{a}) \sim \mathbf{F}_X$ and $\mathbf{Y}(\mathcal{Y}, \mathbf{w}) \sim \mathbf{F}_Y$ as defined in (2) and (1).

2. Compute

$$\mathbf{c}_{\text{opt}} = \arg \min_{\mathbf{c} \in \mathcal{C}_n(m)} d(\mathbf{X}(\mathbf{c}; \mathcal{Y}, \mathbf{a}(\mathbf{c})), \mathbf{Y}(\mathcal{Y}, \mathbf{w})) \quad (5)$$

and return the optimal solution $(\mathbf{c}_{\text{opt}}, \mathbf{a}_{\text{opt}}) = (\mathbf{c}_{\text{opt}}, \mathbf{a}(\mathbf{c}_{\text{opt}}))$

As for ensemble reduction, for many practical problems $\mathcal{C}_n(m)$ is too large to solve the mixed integer problem by brute force.

Note, that in general neither (3), nor (4) and (5) does attain a unique minimum. However, in many applications this is usually the case. Still, if the minimum is not unique, we might report and proceed with all minima or use another decision rule to report only one optimum.

3 Why the energy distance for reduction problems?

There is a wide range of plausible distances/metrics that measure the discrepancy between two random vectors or two multivariate distributions. Potential candidates are the disparity metric, total variation metric, discrepancy metric, Hellinger distance, Wasserstein distances among others. However, as mentioned in the introduction the Wasserstein metric is by far the most popular for scenario reduction. Hence, we recap its definition on \mathbb{R}^k :

$$d_{W,p}(\mathbf{X}, \mathbf{Y}) = \inf_{\gamma \in \Gamma(\mathbf{X}, \mathbf{Y})} \int_{\mathbb{R}^k \times \mathbb{R}^k} \|\mathbf{x} - \mathbf{y}\|_2^p d\gamma(\mathbf{x}, \mathbf{y})$$

where $\Gamma(\mathbf{X}, \mathbf{Y})$ is the set of all probability measures on $\mathbb{R}^k \times \mathbb{R}^k$ with the same marginals as \mathbf{X} on the first k coordinates and the same as \mathbf{Y} on the latter ones. $\Gamma(\mathbf{X}, \mathbf{Y})$ is also known as set of \mathbf{X} and \mathbf{Y} couplings. As mentioned in the introduction, the popularity of the Wasserstein distance in scenario reduction is mainly due to the efficient reduction algorithm proposed introduced in [Dupačová et al. \(2003\)](#). It provides an efficient and explicit formula for the subproblem (5) in scenario reduction. The resulting optimal redistribution rule (see e.g. [Grove-Kuska et al. \(2003\)](#)) corresponds to a (mass) transportation problem. Here, it is important to remark, that this algorithm does not require the explicit computation of the Wasserstein distance which leads to a dramatic speed up compared to alternatives.

Still, also for Wasserstein based scenario reduction, the NP-hard integer-valued optimization problem (4) is remaining. In consequence, in ensemble reduction (3) the advantages of the Wasserstein distance diminish as the optimization step as in (5) is not required.

NP-hard integer-valued subproblem (3) or (4) is usually solved by heuristics for higher dimensional problems. Typically, forward selection (FS), backward selection (FS) or relatives like fast forward selection (FFS) or forward selection in wait-and-see clusters (FSWC) are applied, see e.g. [Grove-Kuska et al. \(2003\)](#); [Römisch \(2009\)](#); [Feng and Ryan \(2013\)](#). However, other alternatives like particle swarm optimization, neural network base deep learning methods and other heuristics are applied too, see [Li and Gao \(2019\)](#).

The Wasserstein distance $d_{W,1}$ with $p = 1$ is often applied to scenario reduction as there exist a useful dual representation of the metric. Also note that in the $k = 1$ -dimensional case the Wasserstein distance $d_{W,1}$ simplifies to

$$d_{W,1}(X, Y) = \int_{\mathbb{R}} |F_X(z) - F_Y(z)| dz \tag{6}$$

which is the L^1 -distance between the two cumulative distribution functions.

A related discrepancy measure to (6) is the Cramér distance. It is given by

$$d_C(X, Y) = \int_{\mathbb{R}} |F_X(z) - F_Y(z)|^2 dz \tag{7}$$

and measures the squared L^2 -distance between the two cumulative distribution functions. Thus, just from the intuition point of view $d_{W,1}$ and d_C should exhibit similar properties. The Cramér distance has a useful different representation given by

$$d_C(X, Y) = \mathbb{E}|X - Y| - \frac{1}{2}\mathbb{E}|X - X'| - \frac{1}{2}\mathbb{E}|Y - Y'| \quad (8)$$

where X' and Y' are iid copies of X and Y .

Now, the interesting part is that the representation (8) allows for a natural generalization of the Cramér distance to \mathbb{R}^k , called energy distance, see [Székely and Rizzo \(2013\)](#). The *energy distance* is defined as

$$d_{E,p}(\mathbf{X}, \mathbf{Y}) = \mathbb{E}\|\mathbf{X} - \mathbf{Y}\|_2^p - \frac{1}{2}\mathbb{E}\|\mathbf{X} - \mathbf{X}'\|_2^p - \frac{1}{2}\mathbb{E}\|\mathbf{Y} - \mathbf{Y}'\|_2^p \quad (9)$$

where $p \in (0, 2)$ and again \mathbf{X}' and \mathbf{Y}' are an iid copy of \mathbf{X} and \mathbf{Y} . Obviously, for $k = 1$ and $p = 1$ (9) corresponds to the Cramér distance. Similarly, the case $p = 1$ is regarded as the standard energy distance for $k > 1$. Moreover, the energy distance is a special case of the maximum mean discrepancy, see e.g. [Borgwardt et al. \(2006\)](#).

As pointed out in [Székely and Rizzo \(2013\)](#); [Szekely and Rizzo \(2017\)](#), the energy distance satisfies all axioms of a metric, especially the energy distance is zero ($d_{E,p}(\mathbf{X}, \mathbf{Y}) = 0$) if and only if \mathbf{X} and \mathbf{Y} share the same distribution (almost surely). Moreover, it has useful transformation properties. So $d_{E,p}$ is scale equivariant, i.e. for all constants $a \in \mathbb{R}$ there is a non-zero real-valued function g such that it holds $d_{E,p}(a\mathbf{X}, a\mathbf{Y}) = g(a)d_{E,p}(\mathbf{X}, \mathbf{Y})$. The energy distance satisfies the condition by choosing $g(z) = z^p$ which makes the choice $p = 1$ to a natural candidate for applications. Furthermore, the energy distance exhibits rotational invariance, i.e. for every orthonormal matrix \mathbf{A} it holds $d_{E,p}(\mathbf{A}\mathbf{X}, \mathbf{A}\mathbf{Y}) = d_{E,p}(\mathbf{X}, \mathbf{Y})$. It is interesting to note, that the multivariate version of (7) results in a measure that is not rotational invariant. This is a hint that (8) is more suitable for a k -dimensional generalizations than (7) which focuses on the distances between the cumulative distribution functions. It also indicates that in higher dimensions the properties of the Wasserstein distance might deviate substantially from the energy distance.

The likely most important property of the energy distance is an alternative representation by characteristic functions. The energy distance can be rewritten as a weighted L^2 -distance of the characteristic functions $\varphi_{\mathbf{X}}$ and $\varphi_{\mathbf{Y}}$ with $\varphi_{\mathbf{X}}(z) = \mathbb{E}(e^{iz' \mathbf{X}})$ and $\varphi_{\mathbf{Y}}(z) = \mathbb{E}(e^{iz' \mathbf{Y}})$:

$$d_{E,p}(\mathbf{X}, \mathbf{Y}) = C_{k,p} \int_{\mathbb{R}^k} \frac{|\varphi_{\mathbf{X}}(z) - \varphi_{\mathbf{Y}}(z)|^2}{\|z\|_2^{k+p}} dz \quad \text{with} \quad C_{k,p} = \frac{\pi^{\frac{k}{2}} \Gamma(1 - \frac{p}{2})}{p 2^p \Gamma(\frac{k+p}{2})} \quad (10)$$

Here, $C_{d,p}$ is a scaling constant which depends only on the dimension d and p . The weight function $\xi(z) = \|z\|_2^{-(k+1)}$ is a polynomial of the Euclidean norm depending on the dimension k . Interestingly, this is the only choice of any continuous function ξ such that the weighted L^2 -distance $C \int_{\mathbb{R}^k} \xi(z) |\varphi_{\mathbf{X}}(z) - \varphi_{\mathbf{Y}}(z)|^2 dz$ between the characteristic functions $\varphi_{\mathbf{X}}$ and $\varphi_{\mathbf{Y}}$ is scale equivariant and rotational invariant.

The characterization by characteristic functions allows the energy distance to serve for powerful tests, see [Rizzo and Székely \(2016\)](#). For instance [Székely and Rizzo \(2013\)](#) show that the energy distance based test for multivariate normality has a high testing power, higher than all commonly used alternatives. Moreover, it can be utilized to test for non-parametric characteristics like symmetry or skewness. Another, very crucial feature is that the energy distance allows the construction of the distance covariance and distance correlation. The latter is a multivariate measure for dependency and can be regarded as a generalization of the Pearson correlation. The distance correlation can be used to construct test for multivariate independence which is a

remarkable on its own. As we want to maintain the dependency structure in the scenario paths properly the energy distance is a suitable candidate for ensemble and scenario reduction.

In general, the considered distances for reduction problems have to be computed. This holds always for the energy distance $d_{E,p}$ and in ensemble reduction also for the Wasserstein distance $d_{W,p}$. The Wasserstein distance (Nguyen (2011)) can be computed by minimum matching and solving the linear program

$$d_{W,p}(\mathbf{X}, \mathbf{Y}) = \arg \min_{\mathbf{q} \in [0,1]^{\{1, \dots, n\} \times \mathbf{c}}} \sum_{(i,j) \in \{1, \dots, n\} \times \mathbf{c}} q_{i,j} \|\mathbf{y}_i - \mathbf{y}_j\|_2^p \quad (11)$$

such that $\sum_{i=1}^n q_{i,j} = w_j$ and $\sum_{j \in \mathbf{c}} q_{i,j} = w_i$. This problem can be solved using standard linear program methods. Gottschlich and Schuhmacher (2014) propose an alternative shortlist method for (11) which is based on the simplex algorithm and allows substantial speed improvements for multiple applications. The energy distance $d_{E,p}$ for \mathbf{Y} and \mathbf{X} as in (1) and (2) can be computed by equation (9):

$$\begin{aligned} d_{E,p}(\mathbf{X}, \mathbf{Y}) &= \frac{1}{nm} \sum_{i=1}^n \sum_{j \in \mathbf{c}} \|w_i \mathbf{y}_i - w_j \mathbf{y}_j\|_2^p \\ &\quad - \frac{1}{2m^2} \sum_{i \in \mathbf{c}} \sum_{j \in \mathbf{c}} \|w_i \mathbf{y}_i - w_j \mathbf{y}_j\|_2^p - \frac{1}{2n^2} \sum_{i=1}^n \sum_{j=1}^n \|w_i \mathbf{y}_i - w_j \mathbf{y}_j\|_2^p \end{aligned} \quad (12)$$

However, in the reduction problems we do not have to compute equation (12), as the latter term remains unchanged for all \mathbf{c} . Thus, it is sufficient to replace $d_{E,p}$ by

$$\text{ES}_p(\mathbf{X}, \mathbf{Y}) = \frac{1}{nm} \sum_{i=1}^n \sum_{j \in \mathbf{c}} \|w_i \mathbf{y}_i - w_j \mathbf{y}_j\|_2^p - \frac{1}{2m^2} \sum_{k \in \mathbf{c}} \sum_{j \in \mathbf{c}} \|w_j \mathbf{y}_j - w_k \mathbf{y}_k\|_2^p \quad (13)$$

which is known as the *energy score* which is popular in forecasting evaluation, see Gneiting and Raftery (2007). In forecasting evaluation similar questions arise, see Gneiting and Raftery (2007). However, here usually one-sided measures are required. So one input is taken as random variable, the other input into the distance is treated as observation in \mathbb{R}^k and as already materialized. Among forecasters the continuous ranked probability score (CRPS) is usually regarded as the suitable 1-dimensional forecasting criterion for distributions. The CRPS is the one-sided counterpart of the Cramér distance (8). Concerning the computation of the energy score, we remark that the terms $\|w_i \mathbf{y}_i - w_j \mathbf{y}_j\|_2^p$ are computed for all i and j then the computation is fast and of order $\mathcal{O}(nm)$.

For scenario reduction the Wasserstein based approaches have the speed advantage due to the mentioned explicit algorithm proposed by Dupačová et al. (2003). Here, the energy distance based method has a speed disadvantage. However, the inner optimization step in (4) turns with (13) to

$$\mathbf{a}(\mathbf{c}) = \arg \min_{\mathbf{a} \in [0,1]^m, \mathbf{a}' \mathbf{1} = 1} \text{ES}_p(\mathbf{X}(\mathbf{c}; \mathcal{Y}, \mathbf{a}), \mathbf{Y}(\mathcal{Y}, \mathbf{w})) \quad (14)$$

$$= \arg \min_{\mathbf{a} \in [0,1]^m, \mathbf{a}' \mathbf{1} = 1} \frac{1}{n} \sum_{i=1}^n \sum_{j \in \mathbf{c}} \|a_i \mathbf{y}_i - w_j \mathbf{y}_j\|_2 - \frac{1}{2m^2} \sum_{i \in \mathbf{c}} \sum_{j \in \mathbf{c}} \|a_i \mathbf{y}_i - a_j \mathbf{y}_j\|_2. \quad (15)$$

which is quadratic program with linear constraints. Even though the matrix $(a_{i,j})_{(i,j) \in \mathbf{c} \times \mathbf{c}}$ is in general not positive definite the problem can be handled efficiently.

4 Applications

In this section we show different applications for ensemble and scenario reduction using the energy distance and the Wasserstein distance for comparison purpose. First we show an ensemble and scenario reduction study on binary trees which gives more fundamental insights. The second application is for real electricity load/demand data which is highly relevant in many power and energy systems applications. However, the considered real data study is mainly for illustration purpose. We do not apply the reduced scenario sets in a subsequent optimization problem.

4.1 Binary tree

We consider an equally weighted binary tree of size $H = 5$ which branches every step by -1 and 1 . Thus, there are $n = 2^H = 2^5 = 32$ paths in the scenario set. Then we apply exact ensemble and scenario reduction to reduce the number of trajectories from $n = 32$ to $m \in \{2, \dots, 5\}$ with respect to the energy distance $d_{E,1}$ and the Wasserstein distance $d_{E,1}$. Note that due to the symmetry of the tree the resulting solutions are usually not unique. Thus, we report only one optimal solution. Figures 3 and 4 show the results for the ensemble and scenario reduction problem. They also provide the optimal trajectories and for the scenario reduction problem the resulting weights. Similarly to the Figure 2 in the introduction, we also report key characteristics for the approximation of the reduced scenario set to the original set of $n = 32$ paths. In detail we report again, the mean absolute error (MAE) of the approximation for the mean μ_t , standard deviation σ_t and difference of the mean $\Delta\mu_t = \mu_t - \mu_{t-1}$.

In Figures 3 and 4 we observe that for $m = 2$, both distances lead to the same optimal solution. However, for $m > 2$ the solutions of the energy distance and the Wasserstein distance deviate for both the ensemble reduction problem and the scenario reduction problem.

For ensemble reduction and $m = 3$ (Fig. 3b and 3f), we observe that both solutions have the same MAE performance with respect to the mean approximation but the energy distance approximates better the variance structure of the tree. For $m = 4$ (Fig. 3c and 3g) the picture is mixed. Here, the energy distance reduction maintains perfectly the mean behavior in contrast to the Wasserstein distance. But, this comes at the cost of a worse capturing of the variance structure. For $m = 5$ (Fig. 3d and 3h) the picture is clear. The energy distance has a better approximation in all considered characteristics. Another fact that can be observed for $m = 5$ is that in the last step from $t = 4$ to $t = 5$ the energy distance captures better the path dependency than the Wasserstein distance. In a binary tree the ratio of branches which go upwards and downwards is equally distributed. As $m = 5$ is odd this can never be perfectly captured in an ensemble reduction. The energy distance reduction selects 3 increasing and 2 decreasing paths from $t = 4$ to $t = 5$. On the other hand, the optimal Wasserstein distance reduction provides 1 increasing trajectory and 4 decreasing trajectories which is an unnecessary bias from the true behavior.

For the scenario reduction (Fig. 4) with $m > 2$ the quantitative measures are even more in favor for the energy distance. Here, in all characteristics the energy distance reduction obtains preferable results. Moreover, we notice that the weights (Fig. 4b, 4c and 4d) of the energy distance are more equally distributed among all paths than for the Wasserstein distance (Fig. 4f, 4g and 4h). This is not automatically an advantage. However, it gives an indication that the energy potentially mixes the scenario properties in a better way.

4.2 Electricity load profiles

As pointed out in the introduction scenario reduction techniques are widely used in power system applications. Thus, we consider some real data examples for energy system data as well.

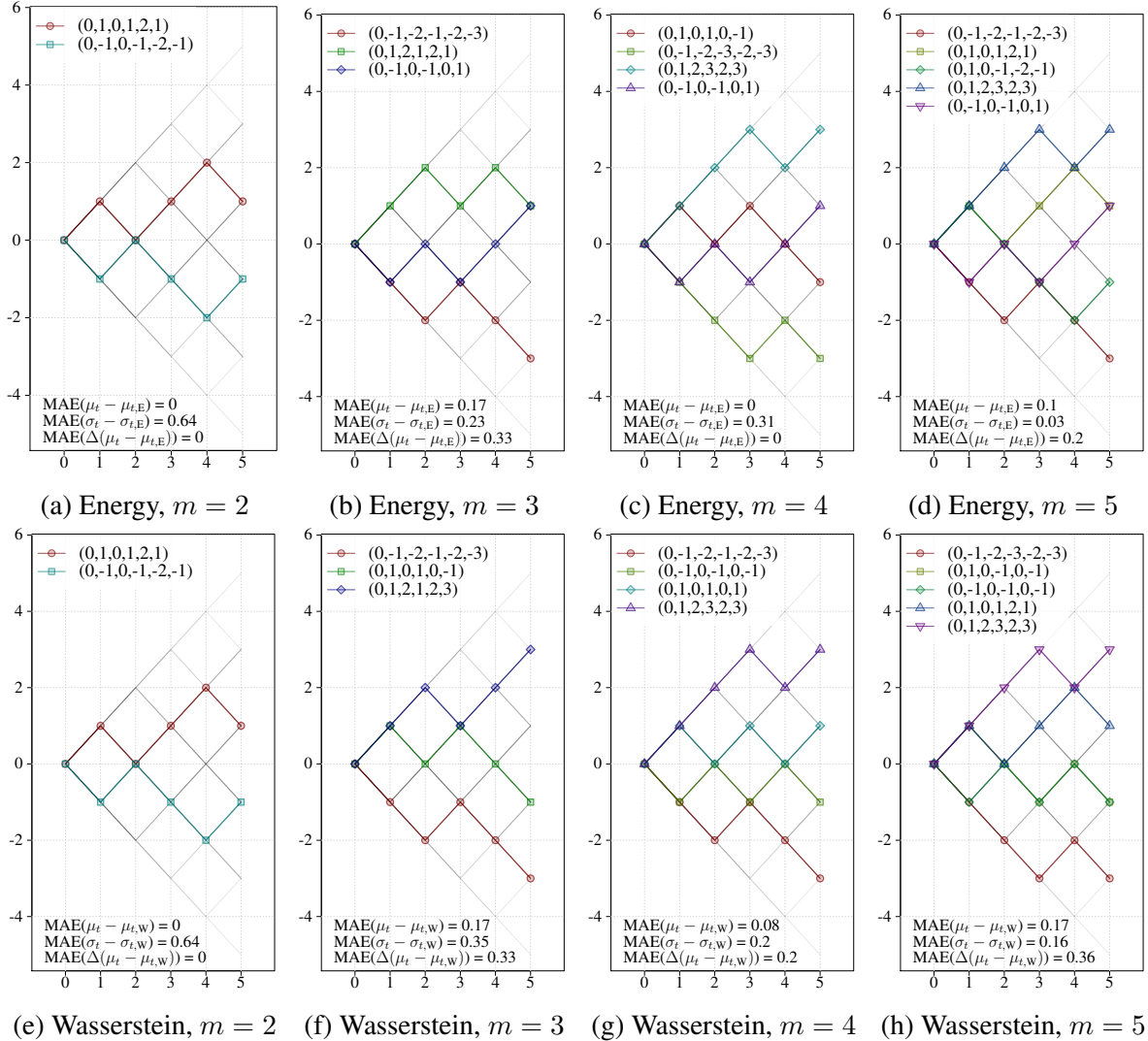


Figure 3: Illustration of exact ensemble reduction for a binary tree of size $H = 5$ and $n = 2^H = 32$ total scenarios. The reduction solutions are performed for $m = 2, \dots, 5$ scenarios (from left to right) for the energy distance $d_{E,1}$ (top row) and the Wasserstein distance $d_{W,1}$ (bottom row). Additionally, the resulting trajectories (top legends) the MAE of the approximation of μ_t , σ_t and $\Delta\mu_t$ are shown (bottom legends).

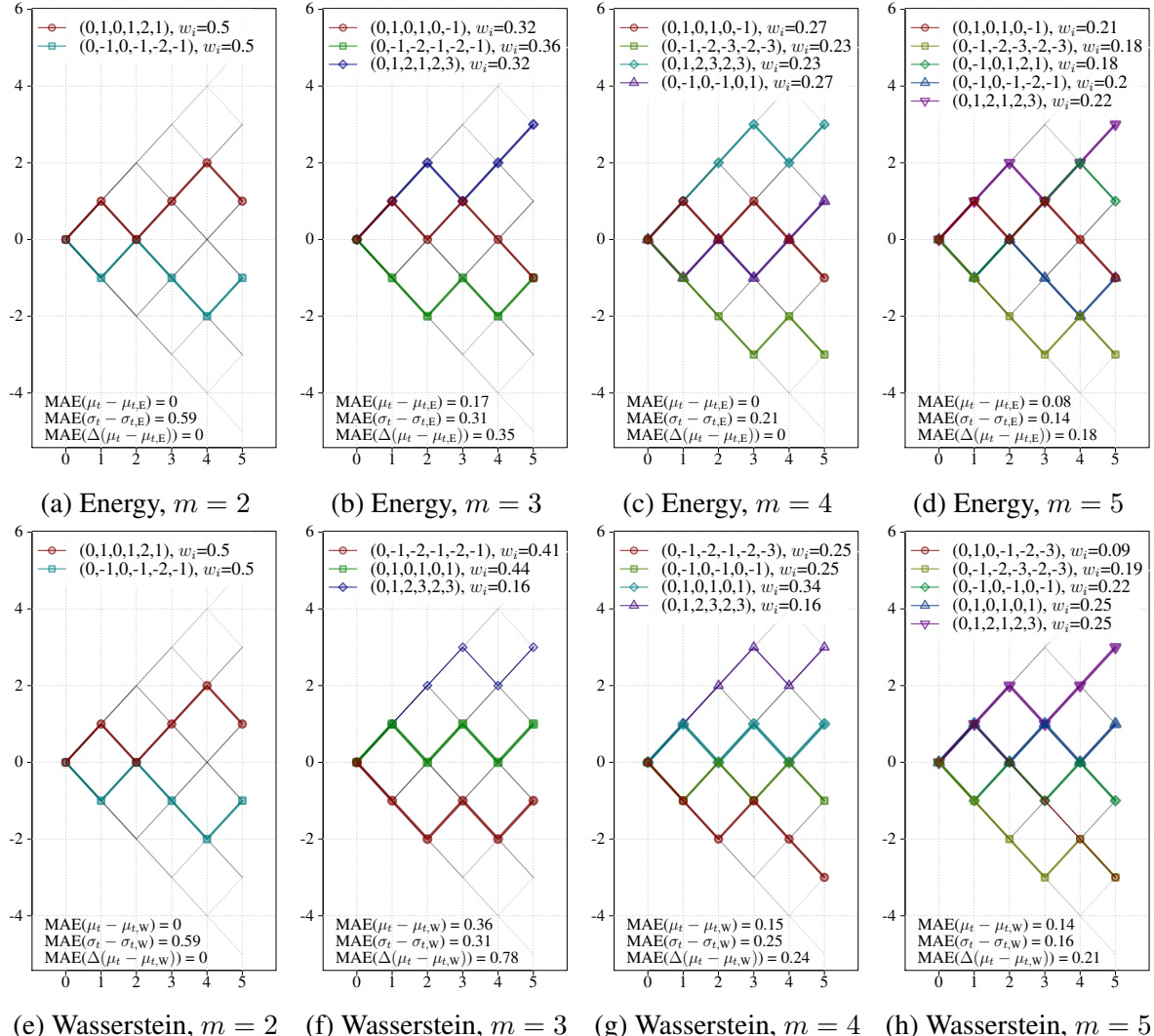


Figure 4: Illustration of exact scenario reduction for a binary tree of size $H = 5$ and $n = 2^H = 32$ total scenarios. The reduction solutions is performed for $m = 2, \dots, 5$ scenarios (from left to right) for the energy distance $d_{E,1}$ (top row) and the Wasserstein distance $d_{W,1}$ (bottom row). Additionally, the resulting trajectories and weights (top legends) the MAE of the approximation of μ_t , σ_t and $\Delta\mu_t$ are shown (bottom legends).

In detail, we consider quarter-hourly German electricity demand data¹ in two different scenario reduction settings. The first application is a small reduction problem where we can consider exact reduction methods. The second application uses forward selection for the scenario reduction and illustrates some characteristics for large reduction problems. In both cases we apply scenario reduction using the energy distance $d_{E,1}$ and the Wasserstein distance $d_{W,1}$.

4.2.1 Exact reduction for demand profiles of 3rd Wednesday of each month.

This illustrative example considers electricity load data from January 2017 to December 2019. For each month the load profile of every 3rd Wednesday of each month is considered as the scenario set. This gives us $3 \times 12 = 36$ historic demand trajectories in total. Exact scenario reduction is computationally feasible, at least for some settings. Note that the consideration of every third 3rd Wednesday in month is sometimes considered in power systems literature as well, see e.g. [Boßmann et al. \(2013\)](#); [Andrychowicz et al. \(2017\)](#).

The considered data and overall results are given in Figure 5. Figures 5a and 5b show the 36 path for the scenario reduction problem and the mean and variance characteristics. Figure 5c to Figure 5j shows the results of exact scenario reduction for the energy and Wasserstein distance with $m = 2, \dots, 5$ reduced scenarios with the same MAE output measure as used before. We observe that the overall behavior is similarly to the binary tree example. The energy distance reduction results tend to have a superior behavior concerning the mean properties. Concerning the capturing of the correct variance structure the results is mixed. For $m = 2$ the Wasserstein distance covers the true variance pattern much better than the energy distance reduction. Vice versa for $m = 3, m = 4$ and $m = 5$ where the energy distance has preferable variance behavior.

Similarly as to the binary tree example we observe that the weights of the energy distance reduction are more equally distributed. For instance for $m = 4$ (Figures 5e and 5i), the Wasserstein distance has a maximum weight of 0.47 for the May'19 trajectory and a minimum weight of 0.14 for the Jan'19 trajectory. In contrast, the energy distance reduction leads to a maximum and minimum weight of 0.30 and 0.21. Thus, we expect more stable and better mixed results from energy distance reductions. Further, we observe that the Wasserstein distance reduction has the tendency to choose slightly more extreme trajectories. Consider e.g. $m = 4$: The Wasserstein distance selected Aug'17 as representative summer trajectory. However, this Aug'17 trajectory has the lowest night load among all considered trajectories in the scenario set. The energy distance selects the Jul'19 path for the representative summer trajectory. This, has a slightly higher overall demand level, also during the night hours. For $m = 3$, we observe a similar selection pattern. The energy distances chooses Dec'18 as representative winter trajectory whereas the Wasserstein distance goes for Jan'19. The latter has a more distinct evening peak.

4.2.2 Forward reduction for demand profiles.

In this scenario reduction application we consider all daily electricity load profiles from 2019 as set of original trajectories. The $n = 365$ trajectories are reduced to $m = 2, \dots, 100$ scenarios. As this reduction problem is computationally not feasible we consider forward selection, see e.g. [Große-Kuska et al. \(2003\)](#). We use simple step forward selection where we add in every iteration one trajectory to the scenario set. This, allows us to compare properties of the reduced set of trajectories with respect to the energy and Wasserstein distance.

Figure 6 presents the setting and the results of the reduction task. The top row (Figures 6a and 6b) illustrate the original set of 365 trajectories with mean and variance characteristics. Figures 6c and 6d illustrates the scenario reduction result for the energy and Wasserstein distance for $m = 10$ final scenarios. They also include the final weights and MAE approximation errors

¹available at <https://transparency.entsoe.eu>

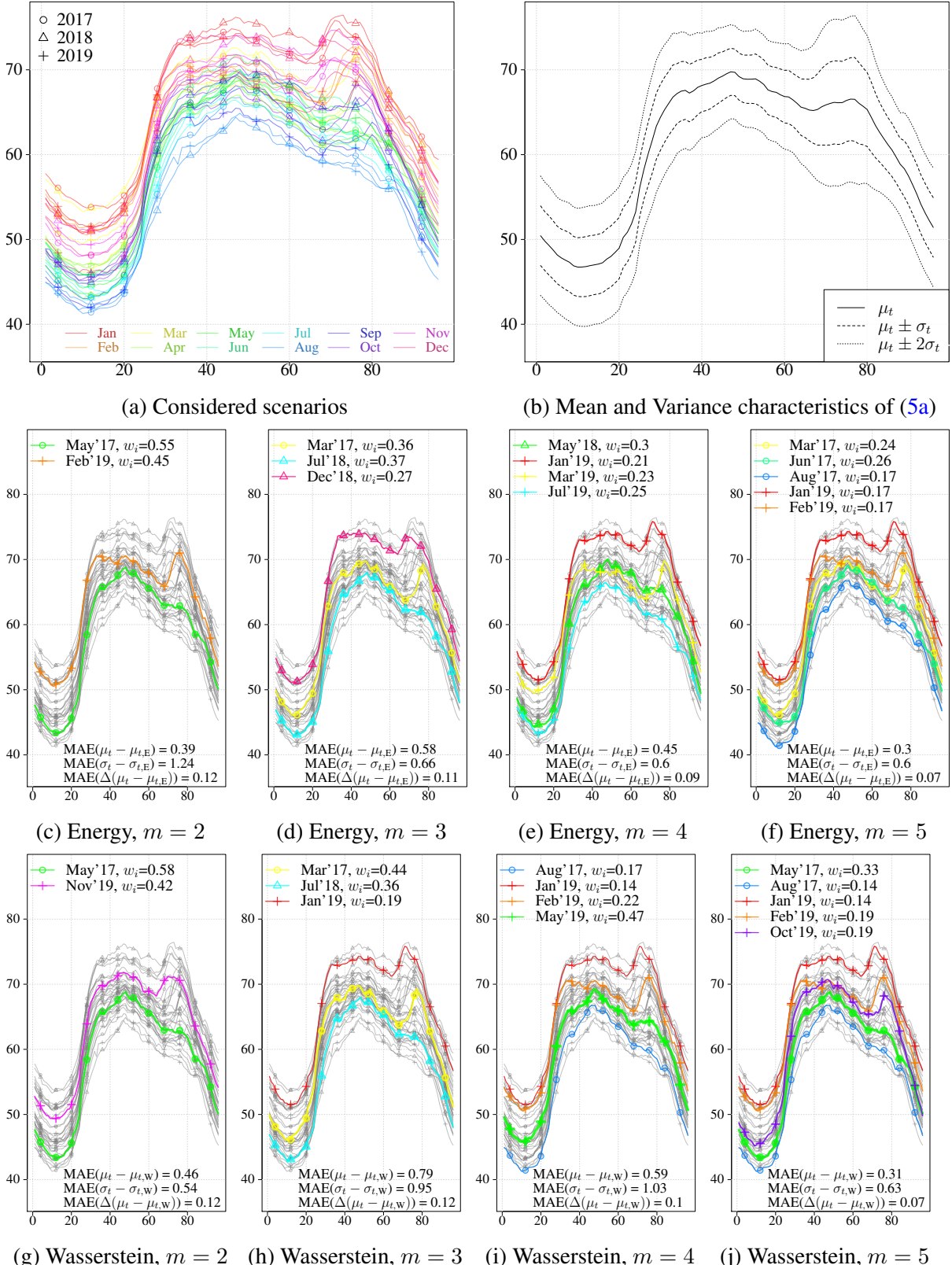


Figure 5: Illustration of exact scenario reduction for electricity demand profiles of Germany [GW] with $n = 36$ total scenarios. The top row shows the $n = 36$ scenarios (top left) with expected value and standard deviation characteristics (top right). The reduction solutions is performed for $m = 2, \dots, 5$ scenarios (from left to right, center and bottom row) for the energy distance $d_{E,1}$ (center row) and the Wasserstein distance $d_{W,1}$ (bottom row). Additionally, the resulting trajectories and weights (top legends) the MAE of the approximation of μ_t , σ_t and $\Delta\mu_t$ are shown (bottom legends).

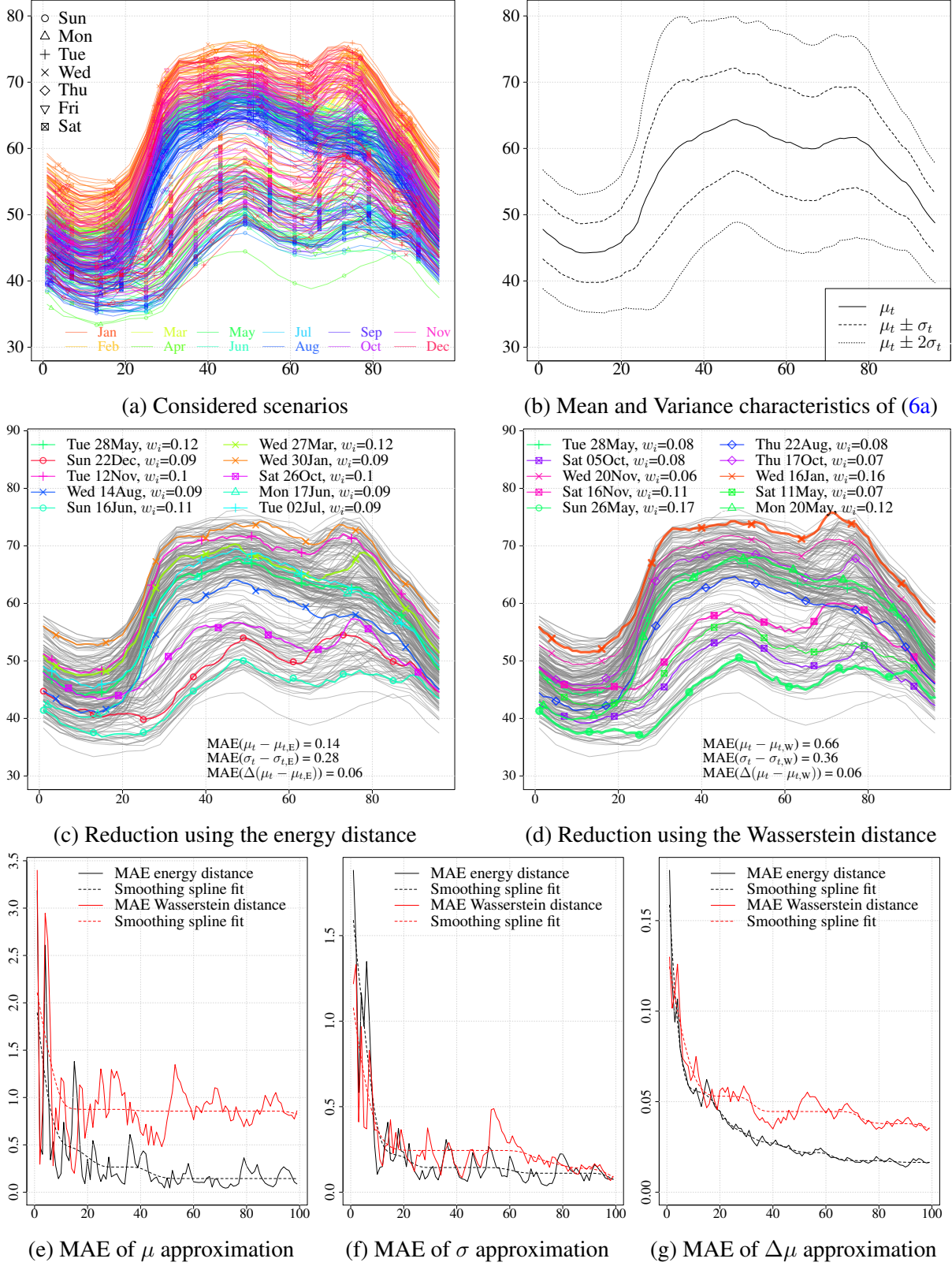


Figure 6: Illustration of scenario reduction using forward selection for electricity demand profiles of Germany [GW] of 2019 with $n = 365$ total scenarios. The top row shows the $n = 365$ scenarios (top left) with expected value and standard deviation characteristics (top right). The reduction solutions for $m = 10$ scenarios for the energy distance $d_{E,1}$ (center left) and the Wasserstein distance $d_{W,1}$ (center right) with characteristics. The bottom row shows the MAE (mean absolute error) of the approximation of μ_t (left), σ_t (center) and $\Delta\mu_t$ (right) for $m = 2, \dots, 100$ scenarios with monotonic smoothing spline fit.

of μ_t , σ_t and $\Delta\mu_t$. Additionally, Figures (6e), (6f) and (6g) depict the three MAE errors for all considered scenario reduction sizes up to $m = 100$. Due to the high variations of the MAEs with respect to m we added a monotonic smoothing spline fit to allow for better interpretation.

First, we interpret the results for $m = 10$ (see 6c and 6d). We observe that the results are similar to the exact reduction results we have seen before. The energy distance seems to provide more equally distributed weights for each trajectory than the Wasserstein distance. The weights vary between 0.09 and 0.12 whereas the Wasserstein distance weights vary between 0.06 and 0.17. Thus, the spread is more than 3 times as high. Moreover, we observe that both methods provide 10 trajectories that cover the general behavior of the data. They include working days and weekend days, such as days in summer and winter. Still, again the energy distance seems to spread the annual characteristic in a better way. The energy distance gives a final set of scenarios that includes days of at least every second month, only February, April, September are missing. On the other hand, the Wasserstein distance misses a representative day from February, March, April, June, July, September and December. That 6 months are not represented is per se not a problem. However, the fact that the period from February to April is not represented can be seen as a bad representation. As we apply forward selection we might also interpret the order of the considered trajectories. We see that both algorithm choose in the first step the same trajectory from Tue 28May but deviate from the second step onwards. A plausible result is that both algorithms choose a weekend day as second trajectory. Concerning the overall weekend representation, the energy distance reduction choose a winter Sunday, a summer Sunday and a fall Saturday whereas the Wasserstein based reduction chooses two fall Saturdays, a spring Saturday and a spring Sunday. Again, the energy distance results seem to be better dispersed. The MAE characteristics draw the same picture: The energy distance provides better mean and variance approximations.

Now, we turn towards the results of the MAE measures for different reduction sizes m (Figures (6e), (6f) and (6g)). We see that everything is possible. Sometimes the Wasserstein distance shows better mean and/or variance statistics than the energy distance, sometimes this is the other way round. In general, we observe that the MAE μ_t , σ_t and $\Delta\mu_t$ approximation errors tend to decrease with increasing m but exhibit strong variations. Only, the MAE of $\Delta\mu_t$ shows a relatively steady reduction in the energy distance case. This result fits the theoretical property that energy distance measures the path dependency better, which is more relevant when evaluation time series differences. In absolute terms we see that for small m the approximation performance is relatively similar for both metrics. The Wasserstein distance is preferable concerning the variance approximation and the energy distance with respect to the mean approximation. Still, for larger m (around $m \geq 10$) the energy distance is most the time better in all considered MAE measures. The superiority of the mean approximation of the energy distance becomes even more distinct for larger m .

5 Discussion and Conclusion

We illustrate that the energy distance is a suitable distance for ensemble and scenario reduction problems. It tends to provide better statistical/stochastic approximation properties than the popular Wasserstein distance which is vastly used in scenario reduction application. This holds particularly for path-dependency properties which are usually relevant in many applications, especially if you think about typical stochastic programs in energy systems like storage, maintenance and power trading optimization.

However, one drawback is that the reduction methods based on the energy distance is computationally more demanding than Wasserstein distance counterpart. This holds especially for the scenario reduction. Here, the Wasserstein distance has a simple explicit solution based on

the redistribution rule which is linked to transportation problems, but the energy distance requires to solve a quadratic program with linear constraints. Still, both metrics give reduction problems are NP-hard and require advanced search algorithms even for moderately sized problems. Sophisticated selection methods that work for the Wasserstein metrics can be applied to the energy distance as well, see e.g. [Li and Gao \(2019\)](#).

From the methodological point of the research can go in different directions. Obviously, we only discussed the energy distance $d_{p,E}$ with $p = 1$ in detail. However, exponents p smaller and larger than 1 are feasible. For heavy tailed data without a finite variance the energy distance with $p < 1$ should provide more better and stable results [Székely and Rizzo \(2013\)](#); [Székely and Rizzo \(2017\)](#).

Moreover, the energy distance can be generalized using kernels to a maximum mean discrepancy (MMD) concept (see e.g. [Borgwardt et al. \(2006\)](#); [Székely and Rizzo \(2017\)](#)). Then the distance measure is given by $\mathbb{E}\kappa(\mathbf{X} - \mathbf{Y}) - \frac{1}{2}\mathbb{E}\kappa(\mathbf{X} - \mathbf{X}') - \frac{1}{2}\mathbb{E}\kappa(\mathbf{Y} - \mathbf{Y}')$ for suitable kernels κ . However, as noted by [Sejdinovic et al. \(2013\)](#) there is no superior kernel κ that serves well in all situations. Furthermore, popular kernels from machine learning like Gaussian or Laplacian kernels suffer disadvantages in high dimensions and do not satisfy scale equivariance, see [Székely and Rizzo \(2017\)](#). Thus, the standard energy distance (see (9)) seems to be a good natural candidate among these class of distances for scenario and ensemble reduction.

Furthermore, the Sinkhorn divergence provides an interesting combination between the energy and Wasserstein distance, see e.g. [Genevay et al. \(2017\)](#); [Bernton et al. \(2017\)](#); [Ramdas et al. \(2017\)](#); [Feydy et al. \(2018\)](#). Here, further investigations with respect to scenario reduction problems might be useful to combine the beneficial properties from both worlds. However, advantage of the low computational complexity of the Wasserstein distance for scenario reduction will be lost.

Finally, we want to remark that we only investigated ensemble and discrete scenario reduction problems but omitted the continuous scenario reduction, see Fig. (1d). Obviously, extensions in this directions might be feasible as well.

References

Andrychowicz, M., Olek, B., and Przybylski, J. (2017). Review of the methods for evaluation of renewable energy sources penetration and ramping used in the scenario outlook and adequacy forecast 2015. case study for poland. *Renewable and Sustainable Energy Reviews*, 74:703–714.

Arpón, S., Homem-de Mello, T., and Pagnoncelli, B. (2018). Scenario reduction for stochastic programs with conditional value-at-risk. *Mathematical Programming*, 170(1):327–356.

Beraldi, P. and Bruni, M. E. (2014). A clustering approach for scenario tree reduction: an application to a stochastic programming portfolio optimization problem. *Top*, 22(3):934–949.

Bernton, E., Jacob, P. E., Gerber, M., and Robert, C. P. (2017). Inference in generative models using the wasserstein distance. *arXiv preprint arXiv:1701.05146*, 1(8):9.

Biswas, P. P., Suganthan, P. N., Mallipeddi, R., and Amaratunga, G. A. (2019). Optimal reactive power dispatch with uncertainties in load demand and renewable energy sources adopting scenario-based approach. *Applied Soft Computing*, 75:616–632.

Borgwardt, K. M., Gretton, A., Rasch, M. J., Kriegel, H.-P., Schölkopf, B., and Smola, A. J. (2006). Integrating structured biological data by kernel maximum mean discrepancy. *Bioinformatics*, 22(14):e49–e57.

Boßmann, T., Pfluger, B., and Wietschel, M. (2013). The shape matters! how structural changes in the electricity load curve affect optimal investments in generation capacity. In *2013 10th International Conference on the European Energy Market (EEM)*, pages 1–8. IEEE.

Davendra, D., Chueh, C.-m., and Hamel, E. (2018). A cuda approach for scenario reduction in hedging models. In *International Conference on Advanced Engineering Theory and Applications*, pages 134–143. Springer.

Di Somma, M., Graditi, G., Heydarian-Foroushani, E., Shafie-Khah, M., and Siano, P. (2018). Stochastic optimal scheduling of distributed energy resources with renewables considering economic and environmental aspects. *Renewable energy*, 116:272–287.

Dupačová, J., Gröwe-Kuska, N., and Römisch, W. (2003). Scenario reduction in stochastic programming. *Mathematical programming*, 95(3):493–511.

Feng, Y. and Ryan, S. M. (2013). Scenario construction and reduction applied to stochastic power generation expansion planning. *Computers & Operations Research*, 40(1):9–23.

Feydy, J., Séjourné, T., Vialard, F.-X., Amari, S.-I., Trouvé, A., and Peyré, G. (2018). Interpolating between optimal transport and mmd using sinkhorn divergences. *arXiv preprint arXiv:1810.08278*.

Gazafroudi, A. (2019). Test. *International Journal of Electrical Power & Energy Systems*, 105:201–219.

Genevay, A., Peyré, G., and Cuturi, M. (2017). Learning generative models with sinkhorn divergences. *arXiv preprint arXiv:1706.00292*.

Glanzer, M. and Pflug, G. C. (2020). Multiscale stochastic optimization: modeling aspects and scenario generation. *Computational Optimization and Applications*, 75(1):1–34.

Gneiting, T. and Raftery, A. E. (2007). Strictly proper scoring rules, prediction, and estimation. *Journal of the American Statistical Association*, 102(477):359–378.

Gottschlich, C. and Schuhmacher, D. (2014). The shortlist method for fast computation of the earth mover’s distance and finding optimal solutions to transportation problems. *PloS one*, 9(10).

Growe-Kuska, N., Heitsch, H., and Romisch, W. (2003). Scenario reduction and scenario tree construction for power management problems. In *2003 IEEE Bologna Power Tech Conference Proceedings*, volume 3, pages 7–pp. IEEE.

Henrion, R., Küchler, C., and Römisch, W. (2009). Scenario reduction in stochastic programming with respect to discrepancy distances. *Computational Optimization and Applications*, 43(1):67–93.

Keko, H. and Miranda, V. (2015). Impact of clustering-based scenario reduction on the perception of risk in unit commitment problem. In *2015 18th International Conference on Intelligent System Application to Power Systems (ISAP)*, pages 1–6. IEEE.

Leou, R.-C., Su, C.-L., and Lu, C.-N. (2013). Stochastic analyses of electric vehicle charging impacts on distribution network. *IEEE Transactions on Power Systems*, 29(3):1055–1063.

Li, Q. and Gao, D. W. (2019). Fast scenario reduction for power systems by deep learning. *arXiv preprint arXiv:1908.11486*.

Nguyen, X. (2011). Wasserstein distances for discrete measures and convergence in nonparametric mixture models. Technical report, Citeseer.

Park, S., Xu, Q., and Hobbs, B. F. (2019). Comparing scenario reduction methods for stochastic transmission planning. *IET Generation, Transmission & Distribution*, 13(7):1005–1013.

Ramdas, A., Trillos, N. G., and Cuturi, M. (2017). On wasserstein two-sample testing and related families of nonparametric tests. *Entropy*, 19(2):47.

Rizzo, M. L. and Székely, G. J. (2016). Energy distance. *wiley interdisciplinary reviews: Computational statistics*, 8(1):27–38.

Römisch, W. (2009). Scenario reduction techniques in stochastic programming. In *International Symposium on Stochastic Algorithms*, pages 1–14. Springer.

Rujeerapaiboon, N., Schindler, K., Kuhn, D., and Wiesemann, W. (2017). Scenario reduction revisited: Fundamental limits and guarantees. *Mathematical Programming*, pages 1–36.

Sejdinovic, D., Sriperumbudur, B., Gretton, A., and Fukumizu, K. (2013). Equivalence of distance-based and rkhs-based statistics in hypothesis testing. *The Annals of Statistics*, pages 2263–2291.

Székely, G. J. and Rizzo, M. L. (2013). Energy statistics: A class of statistics based on distances. *Journal of statistical planning and inference*, 143(8):1249–1272.

Szekely, G. J. and Rizzo, M. L. (2017). The energy of data. *Annual Review of Statistics and Its Application*, 4:447–479.

Wang, J., Shahidehpour, M., and Li, Z. (2008). Security-constrained unit commitment with volatile wind power generation. *IEEE Transactions on Power Systems*, 23(3):1319–1327.

Zhou, Y., Shi, L., and Ni, Y. (2019). An improved scenario reduction technique and its application in dynamic economic dispatch incorporating wind power. In *2019 IEEE Innovative Smart Grid Technologies-Asia (ISGT Asia)*, pages 3168–3178. IEEE.